

Depths of formation of magnetically sensitive absorption lines

V.A. Sheminova

Main Astronomical Observatory, National Academy of Sciences of Ukraine
Zabolotnoho 27, 03689 Kyiv, Ukraine
E-mail: shem@mao.kiev.ua

Abstract

Characteristics of the depression contribution functions are studied for the Stokes line profiles formed in a magnetic field. The form of the depression functions depends mainly on the strength of splitting and the Zeeman component intensity, and is of a complicated character with a distinctly pronounced asymmetry. The depths of formation of magnetically sensitive lines are found by means of these contribution functions. The calculations reveal that the steep section of the line profile is formed higher than the profile center when a strong longitudinal magnetic field is present. The Stokes profiles that describe the polarization characteristics are formed only several kilometers higher than the Stokes profile that specifies the general depression of the unpolarized and polarized radiation. The averaged depth of formation of the whole line profile is practically independent of the magnetic field strength. The depths of formation of 17 photospheric lines usually used in magnetospectroscopic observations are calculated for the models of the quiet photosphere, a flux tube, and the sunspot umbra.

1 Introduction

The determination of depths of formation of the observed Stokes parameter profiles for magnetically sensitive Fraunhofer lines still remains a topical problem of the spectral analysis which is used for obtaining information on the fine structure of magnetic field in the solar photosphere. The problem of the depth of line formation may be considered completely solved for the Fraunhofer lines which are formed in the regions without a magnetic field, in the so-called quiet photosphere, while the present state of the problem dealing with the depths of formation of the Stokes line profiles still remains unsatisfactory.

In observational programs for studying the magnetic field structure in the photospheric layers of the Sun, approximate estimates are usually used for selecting lines with necessary characteristics. Thus, for example, to determine the depth of formation of a Fraunhofer line, its equivalent width is estimated. It is considered that the larger the equivalent width the higher in the atmosphere the line is formed. The magnetic and temperature sensitivity of a line is determined by the value of such atomic parameters of the line as the excitation potential, ionization potential, and Landé factor. The smaller the sum of potentials the more sensitive the line is to the temperature, and the greater the Landé factor the more magnetically sensitive the line is. Though it is possible to get approximate estimates from

such reasonings, more reliable information on the depths of formation of the Fraunhofer line profiles and the Stokes parameter profiles is necessary for a detailed investigation of relationships between the physical parameters of the atmosphere and the depth.

It is not long ago that we have begun the theoretical investigation of the Stokes parameters of magnetically sensitive Fraunhofer lines. The calculation algorithm for the Stokes profiles, for contribution and response functions was developed on the basis of the theory of line formation in a magnetic field for the condition of the local thermodynamic equilibrium; the theory was developed first by Unno and improved by Rachkovskii, Beckers, and Landi Degl'Innocenti. The algorithm and structure of the calculation program SPANSATM can be found in our paper [11]. This program was produced on the basis of the SPANSAT program [1] intended for calculation and analysis of line profiles in stellar atmospheres. The program system SPANSATM enables to carry out the complete analysis of magnetically active photospheric lines in the solar spectrum. Our paper [12] gives the results of investigations of the effect of physical conditions in a magnetic medium and of atomic parameters of lines on the shape of the Stokes profiles and on the magnetic broadening of the Fraunhofer lines. In the present paper, the attention is concentrated mainly on the study of properties of the depression contribution functions and on determination of the depths where the Stokes profiles of photospheric lines are formed. The results of analysis of the response functions of the Stokes parameters will be given in a next paper.

2 Depression contribution functions

When the depths of line formation are calculated, the contribution functions which describe the contribution of atmospheric layers to the observed value of relative absorption in the spectral line are usually used. Besides the contribution functions, the response functions are used in the interpretation of observations. They serve for determination of the response of an observed quantity to a given disturbance. These two functions supplement well each other and together they can give a complete enough information about physical conditions in the medium where spectral line profiles are formed. Depression contribution functions are the functions which show what part of the radiation emerging at the surface (relative to the continuum intensity I_c) is absorbed by each of the atmospheric layers in a given region $\Delta\lambda$ of the spectral line. This function defines the value of the contribution to the relative absorption $R(\Delta\lambda) = [I_c - I(\Delta\lambda)]/I_c$. Here $I(\Delta\lambda)$ is the intensity of the radiation emerging in the region $\Delta\lambda$ of the line. The depression contribution function is equal to zero when the absorption coefficient in the line is zero and the source function in the line S_l is not equal to the intensity of continuous radiation, i.e., S_l should be greater or smaller than I_c . In other words, the depression contribution function is significant if there are atoms which absorb in the given line and the intensities of re-emitted and absorbed radiation are different.

It is no mere chance that we have chosen the depression contribution functions as a tool for investigating the regions where the line absorption processes are localized and for determining the depths of formation of absorption lines. This choice is based on the results of Gurtovenko and Sheminova [5] and conclusions of Magain [8], where a formal solution of the radiation transfer equation was obtained for a relative line depression in the integral form and where the integrand was shown to be the only correct depression contribution function fit for determining the depth of formation of an absorption line. Gurtovenko and Sarychev [4] demonstrate that a depression contribution function proposed earlier which was derived using the Unsöld-Pecker procedure of weight functions is identical to the

depression contribution function from [8]. At present, the depression contribution function proposed first by Gurtovenko, Ratnikova, and de Jager [6] and substantiated theoretically by Magain [8] is widely used in calculating the depths of formation of absorption lines and seems to be beyond any doubt by now.

3 Depression contribution functions of the Stokes parameters

Very few studies have been dedicated to the contribution functions of the Stokes parameters and to depths of their formation due to difficulties in calculations of the Stokes profiles. The depths of formation of the Stokes profiles were studied for the first time by Rachkovskii [10], who compared the variations with depth of the emergent radiation intensities in continuum and in lines and drew the conclusion that the polarization parameters of radiation refer to higher layers than the line intensity does. The contribution functions were already used by Staude [13] to determine the depth of formation of magnetically sensitive lines, but only the contribution to line emission was considered. These studies had some drawbacks – the depths found in them were not the depths of absorption line formation, but characterized the regions of effective radiation in a given line. In order to determine the depth of line formation in the presence of a magnetic field, it is necessary to obtain the depression contribution functions for the Stokes parameters and to calculate the depth of formation, using these functions. The progress in studying the depths of formation of the Stokes parameters began with paper [14] by van Ballegooijen, though the depths of formation were not determined directly there. The method proposed in [14] for solving the transfer equation for polarized radiation enabled to write a single equation in a matrix form instead of four transfer equations for the Stokes parameters; in that equation, the polarized radiation was represented as the matrix

$$\mathbf{D} = \begin{pmatrix} I + Q & U + iV \\ U - iV & I - Q \end{pmatrix},$$

where I , Q , U , V are the Stokes parameters describing the intensity and polarization characteristics of radiation. A formal solution of the transfer equation was obtained in the integral form:

$$\mathbf{D}(0) = \int_{-\infty}^{\infty} \mathbf{C}(\tau) d\tau,$$

where the integrand $\mathbf{C}(\tau)$ is a matrix whose elements define the contribution functions for the Stokes parameters. These contribution functions are called the emission contribution functions of the Stokes parameters. They describe the contribution of radiation of atmospheric layers to the polarized radiation emerging in the line, and the integral of the contribution function along height gives the value of the Stokes parameters. Thus, the author of [14] succeeded in representing each of the Stokes parameters as an integral of an ordinary function along height. This paper stimulated the deriving of the depression contribution functions for the Stokes parameters of the Fraunhofer lines. Grossman-Doerth et al. [2], using the method of [14] and the procedure of [8], were the first to compose the transfer equation for the relative depression of propagating polarized radiation, this depression being represented as the matrix

$$\mathbf{R} = 0.5 \begin{pmatrix} R_I + R_Q & R_U + iR_V \\ R_U - iR_V & R_I - R_Q \end{pmatrix}.$$

The matrix elements in \mathbf{R} contain the Stokes parameters of relative depression: $R_I = 1 - I/I_c$; $R_Q = 1 - Q/I_c$; $R_U = 1 - U/I_c$; $R_V = 1 - V/I_c$. A formal solution of the transfer equation for the matrix \mathbf{R} is the integral

$$\mathbf{R}(0) = \int_{-\infty}^{\infty} \mathbf{C}_{\mathbf{R}}(\tau) d\tau,$$

where the integrand $\mathbf{C}_{\mathbf{R}}(\tau)$ is also a matrix. The depression contribution functions (similar to the emission ones) for each of the Stokes parameters are defined in terms of the $\mathbf{C}_{\mathbf{R}}(\tau)$ matrix elements. Mathematical expressions of the contribution functions for the Stokes parameters can be found in [2, 11]. We used the depression contribution functions [2] for the Stokes parameters in our study to determine the depths of formation of the Stokes profiles of magnetically active absorption lines, denoting them as C_{RI} , C_{RQ} , C_{RU} , C_{RV} in accordance with the Stokes parameters.

4 Characteristic features of the depression contribution functions for the Stokes parameters

In a general case, a spectral line in a magnetic field splits into three groups of components. The first group is characterized by absorption of the radiation polarized linearly in the direction of the magnetic field (the π components). The second group (the σ_r components) is characterized by absorption of the radiation right-hand circularly polarized in the plane perpendicular to the direction of the field. The components of the third group (the σ_b components) are left-hand circularly polarized in the same plane. The observed relative line depression described by the Stokes parameter R_I which represents the absorption of both unpolarized and polarized light in a certain section of the line profile contains information on all the components. The profile of R_I is to be considered as a superposition of profiles of all three component groups. In consequence of this, the function of contribution to the relative depression C_{RI} may be of a complex character. As the contribution function C_{RI} contains contributions of all components, its shape will depend on the spacing between the groups of components and on their intensities. Since the π components remain undisplaced in the magnetic field, the spacing between the σ groups which is determined according to the splitting rule is of importance. The intensities of each group of components depend on the relative selective absorption coefficient at the line center, on the inclination of magnetic field, and on the value of anomalous dispersion. Thus, the contribution function C_{RI} is determined by the effective Landé factor g_{eff} , magnetic field strength, wavelength, number of absorbing atoms, Doppler width, damping constant, magnetic field inclination, etc. The number of parameters is so great that a detailed investigation of contribution functions is very laborious. It seems reasonable to study only characteristic properties of the contribution functions. With that end in view, we calculated the contribution functions for the Stokes parameters of a line and separately for each group of components depending on the profile section $\Delta\lambda$, the inclination angle γ , and the magnetic field strength H . While calculating contribution functions for one group of components, we assumed other functions to be equal to zero. The spectral line Fe I 643.085 nm was selected for calculations. As a model of the region where the line absorption is formed, we took the empirical model of the magnetic flux tube [15] which was obtained by comparing calculated profiles of the Stokes parameters I and an observed line profile in a plage area. The microturbulent velocity was assumed to be 1 km/s, the damping constant was $1.5\gamma_{\text{vdW}}$, and the iron abundance was 7.64 dex.

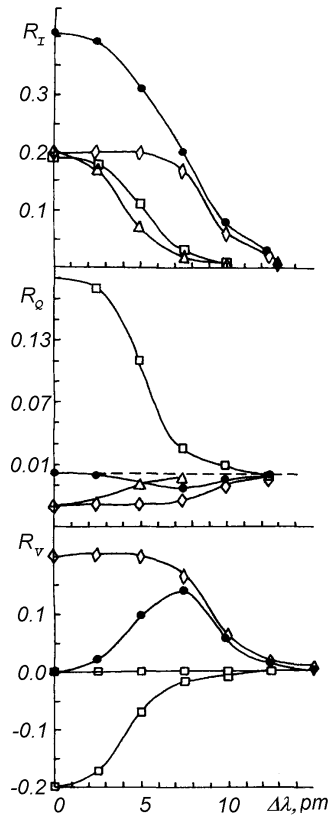


Figure 1: The Stokes profiles of the line Fe I 643.08 nm (points) and its π , σ_b , and σ_r components (squares, triangles, and diamonds, respectively) calculated for model [15].

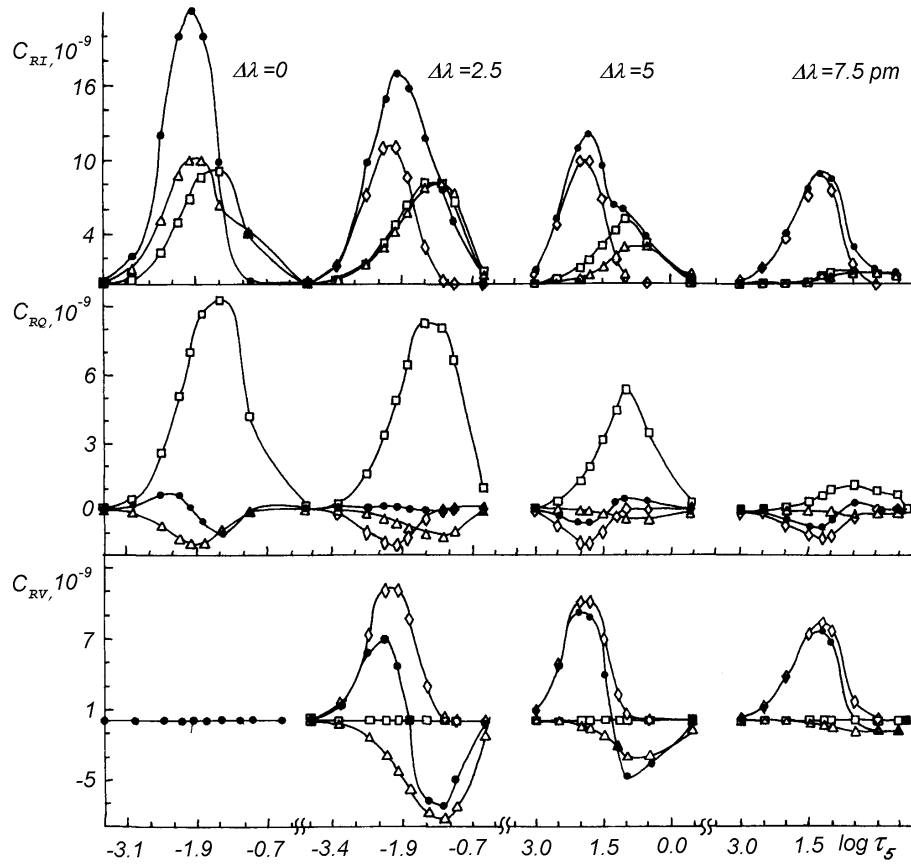


Figure 2: Depression contribution functions of the Stokes parameters for different sections of line profiles (the notation is the same as in Fig. 1).

Analysis of the results obtained revealed a clear dependence of the contribution function profiles for the Stokes parameters on the intensity of the Zeeman components. Figures 1 and 2 show the profiles for the parameters R_I , R_Q , R_V and the corresponding contribution functions C_{RI} , C_{RQ} , and C_{RV} for the line and for its groups of components at different profile sections $\Delta\lambda$ which are formed in a magnetic flux tube with a magnetic field strength of 0.1 T, an inclination of 30° , and an azimuth of 0° . It is evident that the contribution functions for the parameter R_I are asymmetric. A second maximum is outlined in those functions C_{RI} which were calculated for a steep part of the line profile, for $\Delta\lambda = 5$ pm, for example. The contribution functions C_{RI} have a shape close to a symmetric one only for the center and for distant wings of the line. The contribution functions of parameters R_I , R_Q , and R_V can take on the negative values also, as they characterize the difference in absorptions of polarized radiation for two directions. The positive and negative maxima of the C_{RQ} function change places in going from the line center to the wing, which is evidence of a change in the direction of light polarization along the line profile. The positive and negative maxima of the contribution function C_{RV} characterize the predominance of contribution to the absorption of the right-hand and left-hand circularly polarized light, respectively. Their contributions are equal at the line center, and so C_{RV} is equal to zero here. In going to the line wing, the value of the C_{RV} maxima varies in accordance with the contribution of the σ components.

One can see in Figs 3 and 4 how the Stokes profiles R_I , R_Q , R_V and their contribution functions calculated for the profile sections $\Delta\lambda = 0, 5, 10$ pm vary when the inclination increases from 0° to 90° . The function C_{RI} is the most asymmetric for $\gamma = 0^\circ$ and $\Delta\lambda = 5$ pm. The contribution of the undisplaced π component grows with increasing γ . This “smooths” the C_{RI} contribution function, and its asymmetry diminishes. The maximum values of the C_{RQ} function become the greatest at $\gamma = 90^\circ$ and $\Delta\lambda = 5$ pm. The greatest positive and negative maxima of the C_{RV} function are observed at $\gamma = 0^\circ$, $\Delta\lambda = 5$ pm and $\gamma = 60^\circ$, $\Delta\lambda = 5$ pm, respectively.

The effect of the magnetic field strength on the shape of profiles and contribution functions for the sections $\Delta\lambda = 0, 5, 10$ pm is demonstrated in Figs 5 and 6. The profile shape for R_I varies with increasing field strength. The C_{RI} functions for $\Delta\lambda = 0, 5$ pm shift slightly to deeper layers of the atmosphere. Their width increases, and the depression grows for $\Delta\lambda = 10$ pm with growing H , and the values of maxima in the functions C_{RI} grow correspondingly. In the functions C_{RV} , the negative maximum diminishes with increasing H at the same distances from the line center, as the σ group moves away from the line center, and this means that its intensity becomes less at the same $\Delta\lambda$. An increase of the field strength favours a “clearing” of the right-hand polarized absorption from the left-hand polarized one in the right wing of the line profile.

It should be noted that the value of the Landé factor also affects strongly the shape of the contribution functions. The larger g_{eff} the greater is the splitting of components, and the cases are possible when the components separate entirely, i.e., a complete splitting occurs, and then the shape of the contribution functions does not differ from a usual symmetric shape. For example, the complete splitting is observed for the line Fe I 525.02 nm with $g_{\text{eff}} = 3$ which originates in magnetic flux tubes with a longitudinal magnetic field of a strength higher than 0.1 T.

So, variations of the contribution functions of magnetically active absorption lines under the effect of a magnetic field correspond to variations of line profiles. The contribution functions of the Stokes parameter R_I which refer to steep parts of wings of line profiles become asymmetric due to an increase of the distance between splitted line components. A second maximum may appear for moderately strong lines in which $g_{\text{eff}} \geq 2$ when the

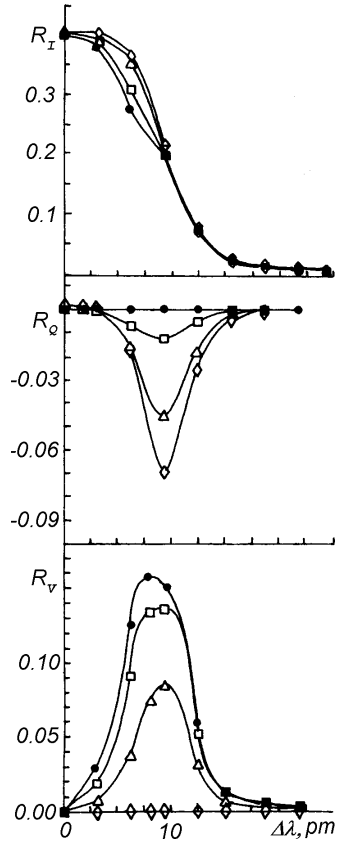


Figure 3: The Stokes profiles of the line Fe I 643.08 nm calculated for model [15] v. inclination: $\gamma = 0^\circ$ (points), 30° (squares), 60° (triangles), 90° (diamonds).

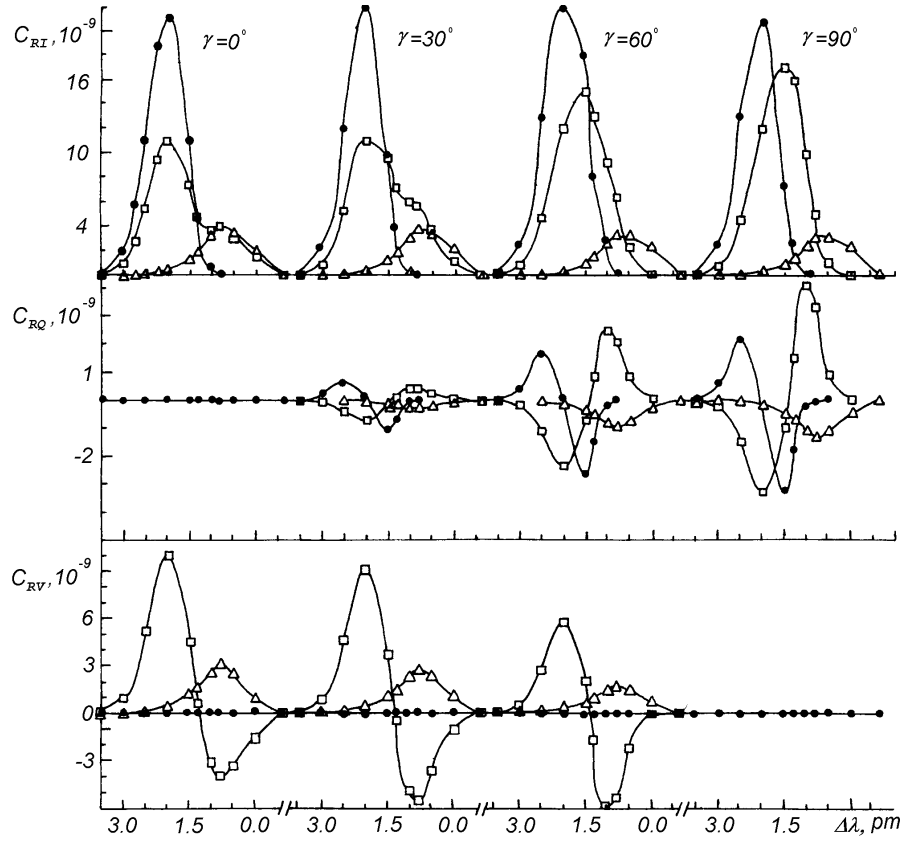


Figure 4: Depression contribution functions of the Stokes parameters for the Fe I 643.08 nm line v. magnetic field inclination for $\Delta\lambda = 0$ (points), 5 pm (squares), 10 pm (triangles).

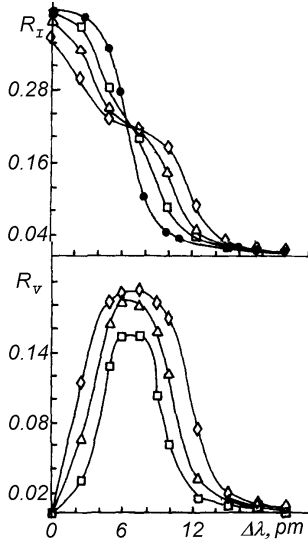


Figure 5: The Stokes profiles of the Fe I 643.08 nm line calculated for the strength $H = 0.0$ T (points), 0.1 T (squares), 0.15 T (triangles), 0.2 T (diamonds) of the longitudinal magnetic field in a magnetic flux tube [15].

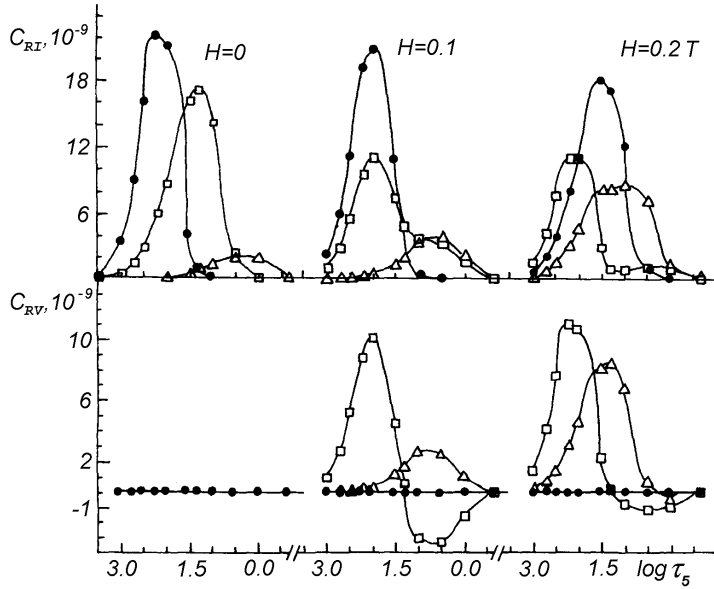


Figure 6: Depression contribution functions of the Stokes parameters for the Fe I 643.08 nm line v. strength of the longitudinal magnetic field for $\Delta\lambda = 0$ (points), 5 pm (squares), 10 pm (triangles).

magnetic field is longitudinal or is close to longitudinal and its strength is higher than 0.1 T. The contribution functions for the polarization parameters R_Q , R_U , and R_V have a complex shape with a positive and a negative maxima.

5 Determining the depth of formation of the R_I Stokes profile.

The mean depth of the layer where the processes of selective absorption in a given frequency interval of a spectral line go effectively is called the depth of formation of the absorption line profile section, and it is calculated as a center of gravity or as a weighted mean value:

$$h(\Delta\lambda) = \int_{-\infty}^{\infty} hF(h, \Delta\lambda)dh / \int_{-\infty}^{\infty} F(h, \Delta\lambda)dh.$$

The depression contribution function is used for the weight function F . The averaging operation is quite justifiable here; this follows from [13], for example, where it is shown that, if a contribution function positive over the whole height interval is normalized, then the new function

$$\varphi(h, \Delta\lambda) = F(h, \Delta\lambda) / \int_{-\infty}^{\infty} F(h, \Delta\lambda) dh$$

thus obtained may be considered as the height distribution of probability density for the given process in the atmosphere. Having calculated the center and variance of the distribution, one can use this function for finding not only the depth but the width also of the layer where a significant contribution occurs. The analysis of the contribution functions for the Stokes parameters made by us has shown that the contribution function for the parameter R_I can be transformed to the probability density function. The depression function C_R is positive and it is easily normalized by dividing it by the value of relative depression $R(\Delta\lambda)$. As a result, we obtain the function

$$\varphi(h, \Delta\lambda) = C_{RI}(h, \Delta\lambda) / R(\Delta\lambda),$$

where

$$R(\Delta\lambda) = \int_{-\infty}^{\infty} C_{RI}(h, \Delta\lambda) dh;$$

this function characterizes the probability of absorption of the unpolarized and polarized radiation in a given line in a given spectral interval $\Delta\lambda$. The depth of formation h_{RI} and the half-width of the effective layer h_{RI} can be calculated now for the parameter R_I by the following expressions:

$$h_{RI}(\Delta\lambda) = \int_{-\infty}^{\infty} h\varphi(h, \Delta\lambda) dh,$$

$$\Delta h_{RI}(\Delta\lambda) = \int_{-\infty}^{\infty} (h - h_{RI})^2 \varphi(h, \Delta\lambda) dh.$$

Besides that, the so-called averaged depth of formation of the complete line profile can be calculated as a weighted mean quantity:

$$h_W = (1/W) \int h_{RI}(\Delta\lambda) R_I(\Delta\lambda) d(\Delta\lambda),$$

where

$$W = \int R_I(\Delta\lambda) d(\Delta\lambda).$$

The relative depression, i.e., the function $R_I(\Delta\lambda)$ is a weight function here; W is the total line depression, or the equivalent width. Calculating the quantities $h_{RI} \pm \Delta h_{RI}$ and h_W by the expressions given here, we define completely the region of formation of the Stokes profile R_I and in that way solve the problem of the depth of formation of a magnetically active absorption line in the presence of a magnetic field.

6 Determining the depths of formation of the polarization line characteristics R_Q , R_U , R_V

The formulae given above cannot be used in this case, since the contribution functions for the Stokes parameters R_Q , R_U , and R_V can take on both positive and negative values

in the height range considered here. In order to find the mean depth of formation of a polarization parameter, it is more convenient to resort to the center of gravity of the plane figure formed by the curve corresponding to the contribution function and by abscissa. For example, let us consider the contribution function C_{RV} for the parameter R_V . The area of the figure S_{RV} is equal to the sum of two areas formed by the positive and negative parts of the C_{RV} curve which lie above and below the abscissa, i.e., $S_{RV} = S_1 + S_2$, where

$$S_1 = \left| \int_{-\infty}^{h_1} C_{RV}(h, \Delta\lambda) dh \right|, S_2 = \int_{h_1}^{\infty} C_{RV}(h, \Delta\lambda) dh,$$

h_1 is the geometric height at which the function C_{RV} changes its sign. We shall use the expression

$$h_{RV} = \int \int h dS_{RV} / S_{RV}$$

to determine the depth of formation of the R_V profile. Substituting the expression for S_{RV} and transforming to a form convenient for calculations, we get

$$h_{RV} = \int_{-\infty}^{\infty} h |C_{RV}(\Delta\lambda)| dh / \int_{-\infty}^{\infty} |C_{RV}(\Delta\lambda)| dh.$$

The depths of formation for the parameters R_Q and R_U can be found in the same way. Thus, to calculate the depths of profile formation for polarization characteristics of magnetically active lines, one can use the formula of weighted mean where the modulus of the depression contribution function of the Stokes parameters is used for the weight function.

7 Investigating depths of formation of the Stokes profiles

Using three lines Fe I 525.02, 523.29, 643.08 nm as an example (Fig. 7), we illustrated the variations in the depth of formation of the Stokes parameters with varying magnetic field strength. We calculated the profiles and the depths of their formation, varying the magnetic field strength H from 0 to 0.2 T. Figure 8 shows the effect of the field inclination on the depth of formation of the Stokes profiles for the line Fe I 643.08 nm. When the inclination varies, the azimuth remains equal to zero, and the field strength is 0.1 T. When calculating the depths of formation of the Stokes profiles, we adopted the magnetic flux tube model of [15] and used the geometric scale height h and the logarithmic optical depth scale $\log \tau_5$, as these scales are mostly used in practice. The depths of formation in the figures are given in the geometric scale height. The geometric height zero level $h = 0$ corresponds to the optical depth $\tau_5 = 1$. Geometric heights below the zero level take on negative values and above it they are positive. Analysis of the results brings us to the following conclusions.

8 On the depth of the layer of the R_I profile effective formation

As is generally known, the Fraunhofer line profiles change their shape in the presence of a magnetic field. It differs from the classic profile shape of a Fraunhofer line (see Fig. 7).

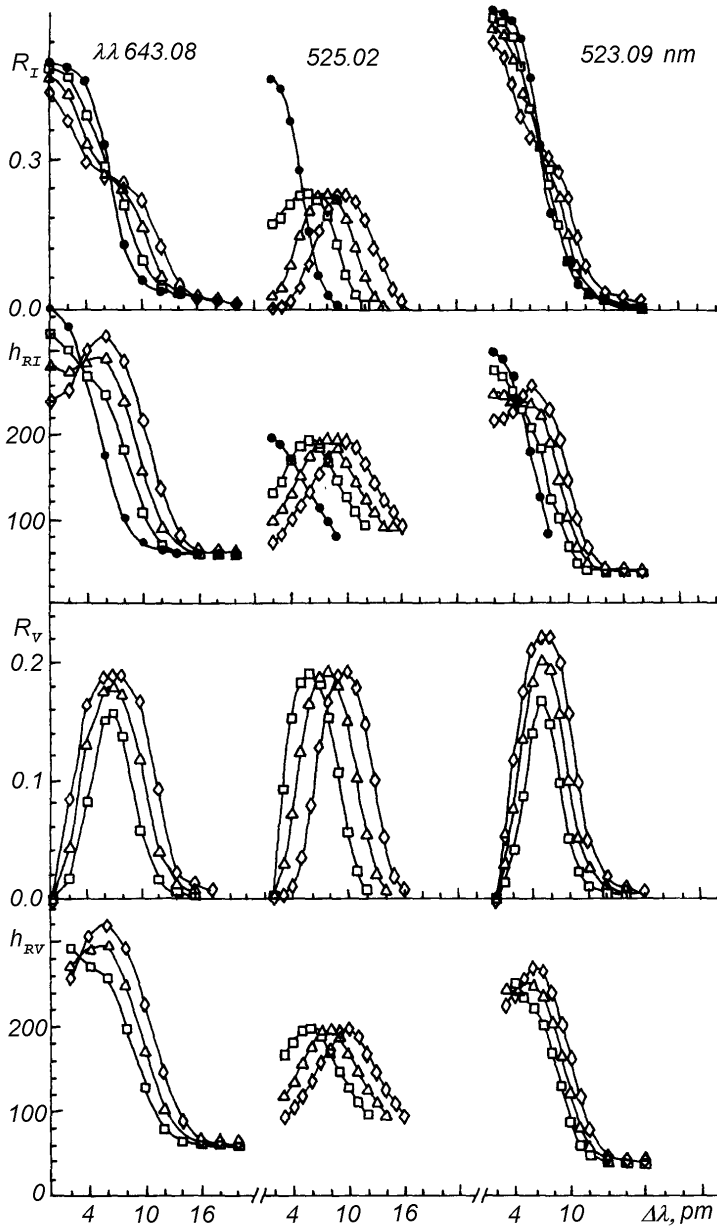


Figure 7: The Stokes parameter profiles of three Fe I lines and depths of their formation h_{RI} and h_{RV} for magnetic field strength $H = 0$ (points), 0.1 T (squares), 0.15 T (triangles), 0.2 T (diamonds) of the longitudinal magnetic field in a magnetic flux tube [15].

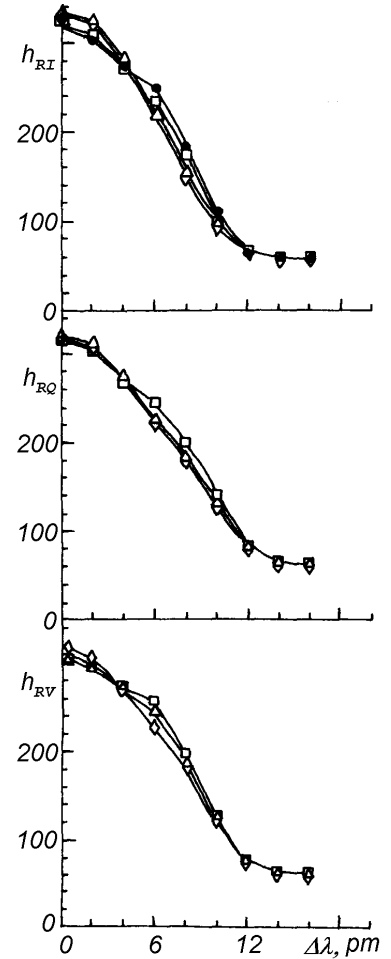


Figure 8: Depths of formation of the Stokes profiles for the Fe I 643.08 nm line v. inclination. For the corresponding Stokes profiles and notation, see Fig. 3.

The depression in the central part of the profile decreases with increasing field strength as compared to the profile calculated without a magnetic field (a “nonmagnetic” profile), and in the line wings it increases. The greater the Landé factor the stronger this effect is. The profiles and the depth of formation of the depression change. It is evident from Fig. 7 that, as the magnetic field strength and the Landé factor are growing, the central part of the profile is formed in more deep layers (the geometric heights decrease), the middle part is formed in more high layers (the geometric heights increase) as compared to the “nonmagnetic” profile, and far wings are formed in the layers where the far wings of “nonmagnetic” profiles are formed. The depth of line formation averaged over the entire profile depends on the manner in which the equivalent width varies. The greater the magnetic broadening of the line the higher in the atmosphere the entire line profile is formed on the average, i.e., the magnetic field as if “forces out” slightly the line upwards. A noticeable growth of the height may be expected for the lines with $g_{\text{eff}} > 2$ and $W > 7.0$ pm for $H > 0.1$ T. But calculations show that this growth is several kilometers only. When magnetic fields are measured from the Fraunhofer lines, it should be remembered that a steep section of the magnetic line profile can form higher in the atmosphere than the profile center. Changes in the magnetic field inclination from 0° to 90° affect little both the profile R_I (Fig. 3) and the depths of its formation (Fig. 8). Appreciable changes are observed only at the distances corresponding to the profile half-widths, where the geometric height of formation decreases with increasing inclination.

9 On the width of the layer of the R_I profile effective formation

The width of the layer where the main fraction of polarized radiation is absorbed in a certain part of line depends on the value of the line splitting in the magnetic field, $\Delta\lambda_H$. When the splitting grows, the layer width also grows. The complete splitting having been reached, the layer width diminishes. The width is different for different parts of the line. The layer width reaches its maximum value, as a rule, for the middle part of the profile wings. The layer width decreases when the magnetic field inclination varies from 0° to 90° . Changes of the layer width that occur under the effect of a magnetic field are as large as tens of kilometers. For example, for a region $\Delta\lambda = 5$ pm in the line Fe I 643.08 nm which is formed in a magnetic flux tube with a field strength of 0, 0.1, 0.15, 0.2, 0.3 T and $\gamma = 30^\circ$, $\varphi = 0^\circ$, the maximum half-width of the effective layer reaches 90, 123, 126, 119, 105 km, respectively. The maximum half-width for inclinations of 0° , 30° , 60° , 90° and $H = 0.1$ T is 123, 116, 100, 92 km, respectively.

10 On the depths of formation of the polarization line characteristics R_Q , R_U , R_V

If the magnetic field is longitudinal, only one polarization parameter R_V exists. The depth of its formation is found to be close to the depth of formation of the R_I profile (Fig. 7). The difference between them reaches several kilometers, R_V being formed slightly higher than R_I . Thus, the depths of formation of the Stokes profiles R_I and R_V for a region $\Delta\lambda = 5$ pm of the lines Fe I 525.02, 523.29, 643.08 nm in a magnetic flux tube with $H = 0.1$ T, $\gamma = 0^\circ$, $\varphi = 0^\circ$ are 187 and 188, 186 and 201, 262 and 267 km, respectively. If the magnetic field

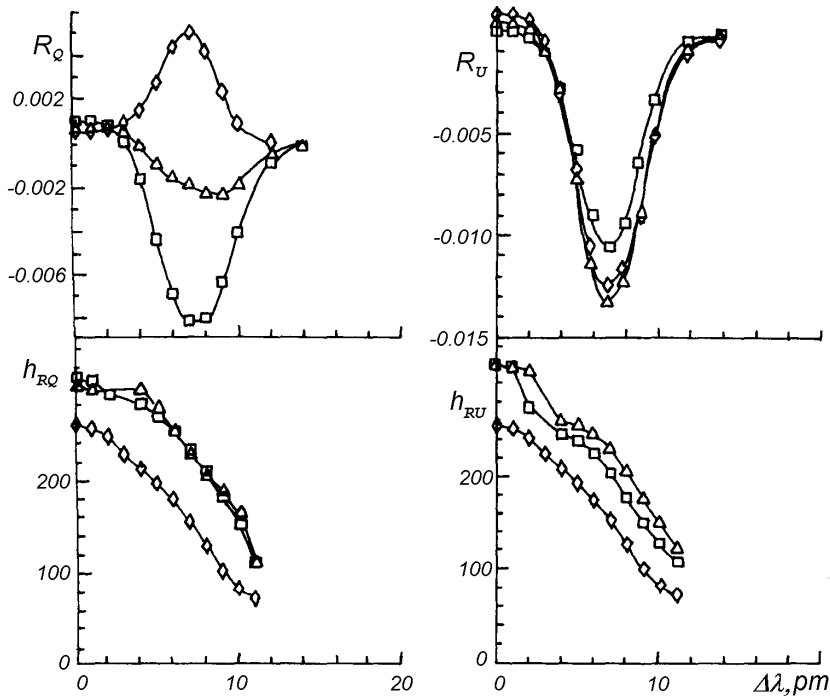


Figure 9: Dependence of the Stokes profiles and depths of formation on azimuth of magnetic field vector: $\varphi = 15^\circ$ (squares), 30° (triangles), 45° (diamonds) for flux tube model [15].

inclination γ varies from 0° to 90° at $\varphi = 0^\circ$, the parameter R_Q appears in addition to R_V , and its profile is formed higher than R_I (Fig. 8). For example, for $\Delta\lambda = 5$ pm of the line 643.08 nm in a magnetic flux tube with $H = 0.1$ T, $\gamma = 30^\circ$, $\varphi = 0^\circ$, the R_I , R_Q , and R_V profiles are formed at depths of 253, 258, 256 km, respectively. If we change the angle φ , the parameter R_U will appear. Figure 9 shows how the depths of formation of R_Q and R_U change in these cases. It follows from the results of calculations that the polarization profiles R_Q , R_U , and R_V are formed higher than the general relative depression of the line, R_I , but the difference is insignificant on the average. Therefore, it may be assumed that all the Stokes profiles are formed in the same layers.

11 The depths of formation of lines frequently used in magnetographic observations

For calculating the depths of line formation, first of all it is necessary to define physical conditions in the region of formation or to specify a model solar atmosphere. It is well known that even the simplest horizontally homogeneous model atmosphere is defined by a large number of parameters which vary with height. The accuracy of calculations depends therefore completely on the accuracy of simulation of the conditions in the atmospheric regions where the processes of absorption line formation go. The calculated depth of line formation refers directly to the specific model used in the calculations. Variations of physical conditions in the atmosphere cause variations of such line parameters as the central intensity, equivalent width, profile shape, and the depth of formation as well. Such a notion as the depth of line formation appears to become more indeterminate and becomes meaningless in inhomogeneous model atmospheres. In this case, it is better to use the concept of the effective region of formation.

To demonstrate the aforesaid, we chose three substantially different models. They are the models of the quiet photosphere (HOLMU [7]), a plage area (WAL2 [15]), and a spot (OBST [9]). Table 1 gives the parameters of the lines used. The chemical element

Table 1: Parameters of spectral lines used in calculations.

Line number (no.)	λ , nm	EP , eV	W_{obs} , pm	R	$\log gf$	g_{eff}
1	480.815 Fe I	3.25	2.74	0.336	-2.69	1.33
2	523.294 Fe I	2.93	21.00	0.803	-1.62	1.30
3	523.462 Fe II	3.22	8.85	0.722	-2.31	0.93
4	524.705 Fe I	0.09	6.04	0.716	-5.03	2.00
5	524.757 Cr I	0.96	7.83	0.749	-1.62	2.50
6	525.021 Fe I	0.12	6.48	0.710	-4.89	3.00
7	609.666 Fe I	3.98	3.91	0.358	-1.85	1.50
8	611.165 V I	1.04	1.09	0.084	-0.68	1.33
9	612.622 Ti I	1.07	2.10	0.222	-1.37	1.25
10	612.897 Ni I	1.68	2.36	0.262	-3.27	1.50
11	615.162 Fe I	2.18	4.85	0.507	-3.37	1.83
12	617.334 Fe I	2.22	6.93	0.622	-2.90	2.50
13	630.252 Fe I	3.69	9.08	0.650	-1.14	2.50
14	630.346 Fe I	4.32	0.47	0.045	-2.67	1.50
15	636.946 Fe II	2.89	2.07	0.172	-4.28	2.10
16	643.085 Fe I	2.18	11.17	0.725	-2.08	1.25
17	673.316 Fe I	4.64	2.74	0.239	-1.51	2.50

abundances were taken according to [3]. The magnetic field is longitudinal with a strength of 0.15 T and the azimuth $\varphi = 0^\circ$. The microturbulent velocity is 1 km/s (macroturbulence was ignored), the damping constant is $1.5\gamma_{vdW}$. Tables 2–5 give the results of calculations for the depths of formation of selected lines for each of the models. Table 2 contains the calculation data for the quiet photosphere without regard to a magnetic field. The values of the following parameters are given for each line: equivalent width W averaged over the entire line profile, depth of formation h_W , optical depth $\log \tau_{5W}$, selected section on the profile $\Delta\lambda$, relative line depression R , parameters R_I and R_V , depth of formation and half-width of the effective layer of the depression $\log \tau_{5RI} \pm \Delta$, $h_{RI} \pm \Delta$, $h_{RV} \pm \Delta$. In order to demonstrate variations in the depth of formation over a profile from one model to another, we selected three sections on the profile calculated for the HOLMU model without a magnetic field: at the line center, at a distance corresponding to the line half-width, and in a wing, where the depression was 1%. Further, the depths of formation were calculated in other models for the same sections $\Delta\lambda$. An additional point on the profile was calculated in that part of the wing where it became wider. The data given in the tables demonstrate clearly the reaction of lines to the conditions of their formation. As an example, we may point at the lines whose equivalent width more than doubled upon the temperature rise. These are the lines V I 611.16 nm, Ti I 612.62 nm, Ni I 612.89 nm, Fe I 524.75, 525.02, 615.16, 617.33, 630.25 nm. The lines Fe II 523.46 and 636.94 nm react weakly to the temperature rise, but they practically disappear when the temperature drops, in a spot, for example. Other conclusions may be also drawn from the data given in the tables, and everyone who is interested in and needs this has such an opportunity.

 Table 2. Depths of line formation. Quiet photosphere model HOLMU. $H = 0$ T.

no.	W , nm	h_W , km	$\log \tau_{5W}$	$\Delta\lambda$, pm	R	$\log \tau_{5} \pm \Delta$		$h \pm \Delta$, km	
1	2.68	166	-1.11	0	0.48	-1.25	0.75	187	116
				3	0.20	-0.98	0.72	145	111
				6	0.12	-0.62	0.59	91	89
2	9.66	296	-1.96	0	0.80	-2.85	0.69	431	104
				5	0.52	-1.22	0.71	183	110
				20	0.01	-0.63	0.53	92	81

Table 2 (continued)

no.	W , nm	h_W , km	$\log \tau_{5W}$	$\Delta\lambda$, pm	R	$\log \tau_5 \pm \Delta$		$h \pm \Delta$, km	
3	8.86	262	-1.74	0	0.78	-2.59	0.79	392	120
				6	0.28	-0.62	0.59	90	89
				17	0.01	-0.34	0.48	50	68
4	6.28	315	-2.08	0	0.77	-2.54	0.85	384	129
				4	0.39	-1.55	0.85	233	130
				8	0.01	-0.97	0.65	143	101
5	7.59	300	-1.98	0	0.78	-2.57	0.74	390	111
				5	0.33	-1.20	0.74	179	115
				11	0.01	-0.76	0.56	111	86
6	6.74	328	-2.17	0	0.79	-2.69	0.84	408	127
				4	0.46	-1.60	0.85	241	131
				8	0.01	-0.96	0.65	142	101
7	3.78	177	-1.18	0	0.48	-1.38	0.73	208	112
				4	0.22	-1.00	0.69	148	107
				9	0.01	-0.56	0.52	82	78
8	1.08	189	-1.26	0	0.17	-1.32	0.78	197	120
				3	0.09	-1.23	0.76	184	118
				6	0.01	-1.05	0.72	156	112
9	2.04	197 -	1.31	0	0.30	-1.40	0.79	210	122
				3	0.17	-1.27	0.77	191	119
				7	0.01	-0.97	0.70	145	108
10	2.30	201	-1.34	0	0.35	-1.44	0.81	217	125
				3	0.19	-1.28	0.79	192	122
				7	0.01	-0.93	0.69	138	106
11	4.83	234	-1.55	0	0.59	-1.81	0.79	274	121
				4	0.30	-1.30	0.77	195	119
				8	0.01	-0.83	0.62	122	96
12	6.97	279	-1.85	0	0.68	-2.33	0.75	353	113
				5	0.35	-1.29	0.76	193	117
				11	0.01	-0.74	0.55	108	85
13	9.30	267	-1.77	0	0.69	-2.51	0.68	380	102
				6	0.37	-1.10	0.67	163	104
				30	0.01	-0.60	0.51	88	78
14	0.45	138	-0.93	0	0.07	-0.97	0.70	144	108
				3	0.04	-0.90	0.69	133	106
				5	0.01	-0.79	0.65	116	100
15	1.99	132	-0.90	0	0.28	-1.00	0.76	148	117
				3	0.17	-0.85	0.73	125	112
				7	0.01	-0.55	0.62	81	93
16	11.83	358	-2.37	0	0.75	-3.46	0.70	522	108
				7	0.42	-1.29	0.72	193	111
				30	0.01	-0.76	0.55	111	85
17	2.72	154	-1.04	0	0.33	-1.18	0.70	176	109
				4	0.16	-0.93	0.67	138	104
				9	0.01	-0.54	0.52	78	77

Table 3. Depths of line formation. Quiet photosphere model HOLMU. $H = 0.15$ T.

no.	W , nm	h_W , km	$\log \tau_{5W}$	$\Delta\lambda$, pm	R_I	$\log \tau_{5RI} \pm \Delta$		$h_{RI} \pm \Delta$, km		R_V	$h_{RV} \pm \Delta$, km	
1	2.69	166	-1.11	0	0.31	-1.08	0.73	161	113	0.00		
				3	0.24	-1.18	0.75	178	116	0.21	187	115
				8	0.01	-0.63	0.59	92	89	0.01	96	92
2	9.76	298	-1.97	0	0.77	-2.40	0.70	365	105	0.00		
				5	0.44	-2.17	0.90	329	136	0.33	336	137

Table 3 (continued)

no.	W , nm	h_W , km	$\log \tau_{5W}$	$\Delta\lambda$, pm	R_I	$\log \tau_{5RI} \pm \Delta$		$h_{RI} \pm \Delta$, km		R_V	$h_{RV} \pm \Delta$, km	
				20	0.01	-0.63	0.53	92	81	0.003	92	81
3	8.88	262	-1.74	0	0.76	-2.33	0.79	354	119	0.00		
				6	0.34	-1.21	0.75	181	116	0.26	196	116
				17	0.01	-0.34	0.48	50	68	0.003	50	68
4	6.46	312	-2.06	0	0.46	-1.62	0.85	244	132	0.00		
				4	0.39	-2.49	0.87	377	132	0.38	382	129
				8	0.19	-1.54	0.85	232	131	0.19	233	131
				12	0.004	-0.95	0.63	140	99	0.002	141	100
5	7.62	300	-1.98	0	0.38	-1.24	0.75	187	116	0.00		
				5	0.40	-2.53	0.77	384	116	0.38	387	115
				11	0.10	-1.04	0.71	155	110	0.09	158	111
				14	0.01	-0.75	0.56	111	87	0.01	111	87
6	6.78	330	-2.18	0	0.09	-1.23	0.78	184	121	0.00		
				4	0.38	-2.40	0.86	364	130	0.38	367	128
				8	0.37	-2.27	0.86	344	131	0.37	345	130
				12	0.02	-1.09	0.73	162	113	0.02	164	114
7	3.97	174	-1.17	0	0.26	-1.06	0.71	158	109	0.00		
				4	0.24	-1.29	0.73	193	113	0.22	203	111
				9	0.07	-0.92	0.68	137	105	0.07	140	106
				12	0.01	-0.60	0.54	87	82	0.01	89	84
8	1.08	189	-1.26	0	0.07	-1.21	4.76	181	118	0.00		
				3	0.09	-1.30	0.78	195	120	0.08	199	120
				6	0.05	-1.25	0.77	187	119	0.05	188	119
				9	0.01	-1.08	0.73	161	113	0.01	162	113
9	2.08	196	-1.31	0	0.15	-1.27	0.77	190	119	0.00		
				3	0.15	-1.36	0.79	204	121	0.13	212	121
				7	0.06	-1.24	0.77	185	118	0.06	187	119
				10	0.01	-1.03	0.72	154	111	0.01	157	112
10	2.33	200	-1.33	0	0.12	-1.22	0.77	182	120	0.00		
				3	0.17	-1.40	0.80	210	124	0.15	214	124
				7	0.09	-1.28	0.79	191	122	0.09	193	121
				10	0.01	-1.05	0.73	156	113	0.01	158	114
11	4.92	233	-1.54	0	0.19	-1.19	0.75	178	117	0.00		
				4	0.29	-1.75	0.80	265	122	0.28	270	120
				8	0.21	-1.44	0.78	217	121	0.21	219	121
				12	0.01	-0.87	0.65	128	100	0.01	131	102
12	6.99	281	-1.86	0	0.11	-1.00	0.70	148	108	0.00		
				5	0.33	-2.16	0.77	327	117	0.33	331	115
				11	0.23	-1.45	0.77	220	119	0.23	221	119
				16	0.01	-0.75	0.56	111	87	0.01	111	88
13	9.20	270	-1.79	0	0.23	-0.88	0.62	129	96	0.00		
				6	0.36	-2.39	0.77	362	116	0.33	364	115
				25	0.01	-0.60	0.51	87	78	0.005	88	78
14	0.44	137	-0.92	0	0.02	-0.85	0.67	125	103	0.00		
				3	0.03	-0.94	0.70	140	108	0.03	145	108
				5	0.03	-0.96	0.70	142	108	0.03	144	108
				9	0.01	-0.83	0.67	123	103	0.01	124	103
15	1.99	132	-0.90	0	0.03	-0.63	0.66	92	99	0.00		
				3	0.08	-0.85	0.73	125	112	0.08	127	112
				7	0.13	-0.97	0.75	144	116	0.13	145	116
				12	0.01	-0.59	0.64	86	96	0.01	87	97
16	12.10	360	-2.38	0	0.71	-2.83	0.72	428	108	0.00		
				7	0.40	-2.68	0.96	405	145	0.31	409	146
				30	0.01	-0.76	0.55	111	85	0.002	112	85
17	2.75	155	-1.04	0	0.02	-0.59	0.55	86	83	0.00		

Table 3 (continued)

no.	W , nm	h_W , km	$\log \tau_{5W}$	$\Delta\lambda$, pm	R_I	$\log \tau_{5RI} \pm \Delta$		$h_{RI} \pm \Delta$, km		R_V	$h_{RV} \pm \Delta$, km	
				4	0.08	-0.93	0.67	137	104	0.08	141	104
				9	0.16	-1.15	0.70	172	109	0.16	173	109
				16	0.01	-0.55	0.53	80	79	0.01	81	79

Table 4. Depths of line formation. Magnetic flux tube model of Walton [15]. $H = 0.15$ T.

no.	W , nm	h_W , km	$\log \tau_{5W}$	$\Delta\lambda$, pm	R_I	$\log \tau_{5RI} \pm \Delta$		$h_{RI} \pm \Delta$, km		R_V	$h_{RV} \pm \Delta$, km	
1	1.42	102	-0.71	0	0.16	-0.69	0.67	99	100	0.00		
				3	0.12	-0.77	0.68	111	101	0.11	121	100
				8	0.01	-0.33	0.60	47	86	0.01	52	89
2	5.71	210	-1.42	0	0.47	-1.71	0.53	252	90	0.00		
				5	0.27	-1.53	0.69	227	111	0.20	234	111
				17	0.01	-0.27	0.53	38	75	0.003	39	75
3	5.94	320	-1.98	0	0.44	-2.77	0.63	461	48	0.00		
				6	0.26	-1.57	0.90	240	157	0.19	255	158
				17	0.01	-0.23	0.57	33	82	0.002	34	83
4	2.60	166	-1.15	0	0.14	-0.93	0.67	134	102	0.00		
				4	0.19	-1.31	0.63	190	99	0.18	193	98
				8	0.06	-0.89	0.68	128	102	0.06	129	102
				10	0.01	-0.69	0.67	98	99	0.01	101	100
5	3.98	187	-1.28	0	0.16	-0.79	0.66	113	99	0.00		
				5	0.23	-1.59	0.57	235	94	0.23	237	93
				11	0.04	-0.62	0.65	89	97	0.04	91	97
				12	0.01	-0.39	0.58	55	83	0.01	56	84
6	2.92	176	-1.21	0	0.03	-0.71	0.68	102	100	0.00		
				4	0.18	-1.28	0.63	185	99	0.18	187	98
				8	0.17	-1.22	0.64	176	99	0.17	177	99
				12	0.01	-0.66	0.67	94	98	0.01	96	99
7	1.92	125	-0.87	0	0.12	-0.79	0.65	113	98	0.00		
				4	0.12	-0.98	0.64	141	98	0.10	151	94
				9	0.04	-0.65	0.65	94	97	0.04	97	97
				12	0.01	-0.40	0.60	56	86	0.01	60	88
8	0.32	118	-0.82	0	0.02	-0.78	0.67	112	101	0.00		
				3	0.03	-0.84	0.67	121	101	0.02	125	101
				6	0.02	-0.81	0.67	117	101	0.02	118	101
9	0.66	122	-0.85	0	0.05	-0.82	0.67	118	101	0.00		
				3	0.05	-0.88	0.67	126	101	0.04	132	100
				7	0.02	-0.80	0.67	115	101	0.02	117	101
10	0.81	129	-0.90	0	0.04	-0.82	0.68	117	101	0.00		
				3	0.06	-0.93	0.67	134	102	0.05	138	101
				7	0.03	-0.86	0.67	124	102	0.03	124	102
				10	0.01	-0.72	0.67	103	100	0.01	105	100
11	2.01	149	-1.03	0	0.07	-0.79	0.67	114	100	0.00		
				4	0.13	-1.15	0.63	166	98	0.12	169	96
				8	0.08	-0.97	0.65	140	99	0.08	141	99
				12	0.004	-0.53	0.63	74	91	0.004	78	93
12	3.30	183	-1.26	0	0.04	-0.64	0.65	92	96	0.00		
				5	0.17	-1.41	0.58	206	94	0.17	209	93
				11	0.11	-1.09	0.63	157	97	0.12	158	96
				14	0.01	-0.51	0.62	73	90	0.01	75	91
13	4.95	203	-1.38	0	0.11	-0.66	0.60	93	89	0.00		
				6	0.21	-1.78	0.59	265	99	0.19	267	98
				20	0.01	-0.31	0.53	44	75	0.01	45	75
14	0.19	94	-0.66	0	0.01	-0.58	0.66	83	97	0.00		
				3	0.01	-0.68	0.67	97	99	0.01	101	100

Table 4 (continued)

no.	W , nm	h_W , km	$\log \tau_{5W}$	$\Delta\lambda$, pm	R_I	$\log \tau_{5RI} \pm \Delta$		$h_{RI} \pm \Delta$, km		R_V	$h_{RV} \pm \Delta$, km	
15	1.49	160	-1.08	5	0.02	-0.69	0.67	98	100	0.01	101	100
				7	0.01	-0.64	0.67	92	99	0.01	93	99
				0	0.02	-0.74	0.81	109	128	0.00		
				3	0.06	-1.02	0.82	151	133	0.06	153	133
				7	0.09	-1.18	0.82	175	134	0.09	176	134
16	6.11	252	-1.68	12	0.01	-0.68	0.81	100	125	0.01	101	126
				0	0.39	-1.90	0.49	284	87	0.00		
				7	0.22	-1.82	0.64	273	107	0.18	278	106
				20	0.01	-0.42	0.55	59	79	0.003	61	79
17	1.35	117	-0.82	0	0.01	-0.36	0.58	52	83	0.00		
				4	0.04	-0.71	0.65	02	96	0.04	107	96
				9	0.08	-0.93	0.64	33	97	0.07	134	96
				14	0.01	-0.47	0.62	67	89	0.01	69	90

Table 5. Depths of line formation. Solar sunspot umbra model of Obridko and Staude [9]. $H = 0.15$ T.

no.	W , nm	h_W , km	$\log \tau_{5W}$	$\Delta\lambda$, pm	R_I	$\log \tau_{5RI} \pm \Delta$		$h_{RI} \pm \Delta$, km		R_V	$h_{RV} \pm \Delta$, km	
1	3.30	33	-0.54	0	0.32	-0.62	0.67	39	40	0.00		
				3	0.25	-0.71	0.72	44	44	0.16	56	43
				8	0.04	-0.04	0.44	2	29	0.02	4	30
				14	0.01	0.02	0.43	-2	28	0.003	-2	29
2	16.12	64	-1.08	0	0.73	-2.11	0.73	125	40	0.00		
				5	0.52	-1.63	0.98	98	56	0.21	99	58
				70	0.01	-0.07	0.51	3	33	0.001	15	55
3	0.33	-7	0.08	0	0.04	0.07	0.48	-6	32	0.00		
				5	0.01	0.18	0.43	-13	29	0.01	-11	29
4	17.15	123	-2.11	0	0.81	-2.91	0.83	168	46	0.00		
				4	0.50	-3.88	1.11	224	68	0.37	224	68
				8	0.50	-2.24	1.18	131	67	0.29	134	68
				60	0.01	-0.35	0.60	22	37	0.001	22	37
5	33.27	93	-1.59	0	0.79	-2.61	0.74	152	39	0.00		
				4	0.48	-4.24	0.80	243	50	0.39	243	51
				8	0.55	-3.24	1.17	185	65	0.32	186	65
				81	0.03	-0.33	0.55	20	35	0.004	22	34
6	18.60	118	-2.03	0	0.56	-1.39	0.75	85	42	0.00		
				5	0.45	-4.19	0.81	242	55	0.40	242	55
				11	0.39	-1.55	0.93	93	53	0.25	99	54
				70	0.01	-0.34	0.59	21	37	0.001	22	37
7	2.54	35	-0.56	0	0.14	-0.53	0.63	33	39	0.00		
				4	0.14	-0.72	0.68	44	41	0.10	54	40
				9	0.05	-0.33	0.57	21	36	0.04	27	36
				16	0.01	-0.04	0.44	2	29	0.004	3	29
8	9.54	108	-1.84	0	0.60	-2.02	0.83	120	45	0.00		
				3	0.49	-2.33	1.14	136	63	0.25	138	65
				6	0.39	-2.17	1.00	127	55	0.29	130	55
				30	0.01	-0.40	0.57	25	35	0.002	25	35
9	14.85	116	-1.98	0	0.75	-2.87	0.74	165	39	0.00		
				3	0.64	-2.70	1.18	155	64	0.17	155	68
				7	0.46	-2.28	1.10	133	61	0.27	135	62
				50	0.01	-0.43	0.57	27	35	0.001	28	35
10	3.29	64	-1.05	0	0.18	-0.84	0.79	52	47	0.00		
				3	0.21	-1.23	0.87	75	50	0.18	83	48
				7	0.13	-0.99	0.82	61	48	0.12	64	47
				14	0.01	-0.24	0.53	15	34	0.003	15	34
11	7.15	80	-1.32	0	0.31	-0.96	0.70	59	41	0.00		

Table 5 (continued)

no.	W , nm	h_W , km	$\log \tau_{5W}$	$\Delta\lambda$, pm	R_I	$\log \tau_{5RI} \pm \Delta$		$h_{RI} \pm \Delta$, km		R_V	$h_{RV} \pm \Delta$, km	
				4	0.34	-1.80	0.93	107	53	0.26	110	53
				8	0.26	-1.42	0.82	86	47	0.22	90	46
				26	0.01	-0.20	0.51	12	33	0.003	13	33
12	10.53	86	-1.44	0	0.25	-0.70	0.56	43	34	0.00		
				5	0.38	-2.12	1.01	124	57	0.29	126	57
				11	0.27	-1.36	0.79	83	45	0.22	87	45
				43	0.01	-0.20	0.50	12	33	0.003	13	32
13	9.61	60	-0.99	0	0.21	-0.55	0.46	35	29	0.00		
				6	0.33	-1.63	0.86	98	50	0.24	100	50
				47	0.01	-0.07	0.46	4	30	0.003	5	30
14	0.15	23	-0.37	0	0.01	-0.25	0.58	15	37	0.00		
				3	0.01	-0.40	0.66	25	41	0.10	32	42
				6	0.01	-0.39	0.65	24	41	0.01	28	41
15	0.004	-4	0.04	0	0.0001	0.17	0.43	-12	29	0.00		
				3	0.0003	0.05	0.53	-5	35	0.0003	-4	36
				5	0.0006	0.01	0.56	-2	37	0.0000	-1	37
16	23.30	93	-1.57	0	0.73	-2.97	0.77	172	44	0.00		
				7	0.52	-2.45	1.21	143	68	0.23	144	69
				80	0.02	-0.24	0.51	15	33	0.001	16	33
17	0.99	26	-0.42	0	0.02	-0.98	0.45	6	29	0.00		
				4	0.03	-0.33	0.58	21	37	0.02	27	37
				9	0.05	-0.57	0.66	35	40	0.05	38	40
				16	0.01	-0.07	0.45	4	29	0.01	5	29

12 Conclusion

The depression contribution functions for the Stokes parameters of magnetically active absorption lines are of a complex nature in the conditions of the solar atmosphere in the regions where a strong magnetic field is present. The depression functions may be considered as a result of combining the contribution functions of groups of the components into which a line splits in a magnetic field. The function profiles depend to a large extent on the value of splitting $\Delta\lambda_H$ and on the intensity of each of the components. The depression functions may be used to determine the depth and width of the effective layer where the Stokes profiles are formed.

The profiles of the line polarization parameters are formed several kilometers higher than the profile of the parameter which describes the general depression of polarized and unpolarized radiation. The Stokes profiles may be considered to form in the same layer due to a small difference between the depths of their formation. Magnetically active lines with large values of the Landé factor which form in the presence of a strong longitudinal magnetic field have a distinctive feature – the steep section of the line profile is formed higher than the center of the line profile.

The averaged depth of line formation depends on the amount for magnetic broadening. When the latter increases, the whole region of line formation shifts slightly into the layers lying higher. This effect being insignificant, the averaged depth of line formation in a magnetic field does not change.

It is not possible to draw up tables of calculated depths of formation of magnetically active lines on account of a strong dependence of the value of depression and the depth of line formation on physical conditions in the medium. The depths of formation should be calculated every time the conditions in the medium change.

References

- [1] A. S. Gadun and V. A. Sheminova, SPANSAT: Program for Calculating Spectral Absorption Line Profiles in Stellar Atmospheres in the LTE Approximation [in Russian], Kiev, 1988 (Institute of Theoretical Physics AS Ukr SSR Preprint ITF-88-87P).
- [2] U. Grossman-Doerth, B. Larsson, and S. K. Solanki, “Contribution and response functions for Stokes line profiles formed in a magnetic field,” *Astron. and Astrophys.*, vol. 204, no. 1, pp. 266–274, 1988.
- [3] E. A. Gurtovenko and R. I. Kostyk, *The Fraunhofer Spectrum and the System of Solar Oscillator Strengths* [in Russian], Nauk. Dumka, Kiev, 1989.
- [4] E. A. Gurtovenko and A. P. Sarychev, “Solving the transfer equation for absorption and the depth of formation of the Fraunhofer lines,” *Astron. Zhurn.*, vol. 65, no. 3, pp. 653–655, 1988.
- [5] E. A. Gurtovenko and V. A. Sheminova, “Once more on the depth of formation of the Fraunhofer lines,” *ibid.*, vol. 60, no. 5, pp. 982–994, 1983.
- [6] E. A. Gurtovenko, V. A. Ratnikova, and C. de Jager, “On the average optical depth of formation of weak Fraunhofer lines,” *Solar Phys.*, vol. 37, no. 1, pp. 43–52, 1974.
- [7] H. Holweger and E. A. Muller, “The photospheric barium spectrum: solar abundance and collision of BaII lines by hydrogen,” *ibid.*, vol.39, no. 1, pp. 19–30, 1974.
- [8] P. Magain, “Contribution functions and the depth of formation of spectral lines,” *Astron. and Astrophys.*, vol. 163, no. 1/2, pp. 135–139, 1986.
- [9] V. N. Obridko and J. Staude, “A two-component working model for a large sunspot umbra,” *ibid.*, vol. 189, no. 1, pp. 232–242, 1988.
- [10] D. N. Rachkovskii, “Formation of absorption lines in an inhomogeneous magnetic field,” *Izv. Krym. Astrofiz. Observatorii*, vol. 40, pp. 127–137, 1969.
- [11] V. A. Sheminova, *Calculating Profiles of the Stokes Parameters of Magnetically Sensitive Absorption Lines in Stellar Atmospheres* [in Russian], Kiev, 1990 (VINITI File No. 2940–V90, 30 May 1990).
- [12] V. A. Sheminova, *Effect of Physical Conditions in the Medium and of Atomic Constants on the Stokes Profiles of Absorption Lines in the Solar Spectrum* [in Russian], Kiev, 1991 (Institute of Theoretical Physics AS Ukr SSR Preprint ITF-90-87P).
- [13] J. Staude, “On the mean depth of line formation in a magnetic field,” *Solar Phys.*, vol. 24, no. 2, pp. 255–261, 1972.
- [14] A. A. van Ballegooijen, “Contribution functions for Zeeman-split lines and line formation in photospheric faculae,” in: *Measurements of Solar Vector Magnetic Fields*, M. J. Hagyard (Editor), NASA Conf. Publ. 2374, pp. 322–334, 1985.
- [15] S. R. Walton, “Flux tube models of solar plages,” *Astrophys. J.*, vol. 312, no. 3, pp. 909–929, 1987.